

## Supplementary Materials

### Brain pathology recapitulates physiology: A network meta-analysis

Thomas J. Vanasse<sup>†,1</sup>, Peter T. Fox<sup>†,2,3,4\*</sup>, P. Mickle Fox<sup>2</sup>, Franco Cauda<sup>5</sup>, Tommaso Costa<sup>5</sup>,  
Stephen M. Smith<sup>6</sup>, Simon B. Eickhoff<sup>7,8</sup>, Jack L. Lancaster<sup>2,3</sup>

<sup>1</sup>Department of Psychiatry, University of Wisconsin-Madison, Madison, Wisconsin, USA

<sup>2</sup>Research Imaging Institute, University of Texas Health Science Center at San Antonio, San Antonio, Texas, USA

<sup>3</sup>Department of Radiology, University of Texas Health Science Center at San Antonio, San Antonio, Texas, USA

<sup>4</sup>South Texas Veterans Health Care System, San Antonio, Texas, USA

<sup>5</sup>FocusLab and GCS-fMRI, University of Turin and Koelliker Hospital, Turin, Italy

<sup>6</sup>Wellcome Centre for Integrative Neuroimaging (WIN FMRI), Oxford University, Oxford, United Kingdom

<sup>7</sup>Institute of Systems Neuroscience, Medical Faculty, Heinrich Heine University Düsseldorf, Düsseldorf, Germany

<sup>8</sup>Institute of Neuroscience and Medicine, Brain & Behaviour (INM-7), Research Centre Jülich, Jülich, Germany

<sup>†</sup>These authors contributed to the work equally.

\*Corresponding Author: Peter T. Fox

Email: [fox@uthscsa.edu](mailto:fox@uthscsa.edu)

## Supplementary Methods

**Spatial Correlation Statistical Inference.** To identify the statistical significance of spatial correspondence between any VBM and FUNCTIONAL ICA component pair, we employed a family-wise error (FWE) strategy based on that of Smith et al.<sup>1</sup>. To create an empirical null distribution, 1,000 iterations of noise simulations were performed. For each iteration, we used our 19 non-artifactual VBM ICA images (real data) and ran spatial correlations to 20 Gaussian noise images that were smoothed with a Gaussian filter matching the FWHM estimate (using `fsl_smoothest` function) for the functional component images. This procedure created a correlation matrix of 19x20. The maximum correlation of the entire correlation matrix was logged for each iteration. This approach of using the maximum of the correlation matrix as a correspondence statistic provides family-wise control for multiple comparisons<sup>2,3</sup>. The number of simulated  $r$  coefficients greater than some threshold divided by the total number of iterations thus provides a p-value.

Our chosen spatial correlation threshold of  $r = 0.31$  corresponds to  $p=0.01$ , family-wise error (FWE) rate corrected. Furthermore, if there was a large discrepancy between two or more components as possible candidates for a match to one component ( $\Delta r > 0.20$ ), then only the stronger association was considered a match because clear fractionation could not be concluded.

**Component Weights and Scaling (per Behavior/Disease Category).** In Figure 4, metadata categories with relatively high component loadings were selected to showcase those that strongly contributed to an independent component's generation.  $N = 20$  (of 56) Behavior Domains and  $N = 29$  (of 43) ICD-10 Diseases were chosen to display. The metadata association matrices were separated into Behaviors ( 13/20 TA-FC networks that matched to VBM ICA components), and Diseases (14/20 VBM ICA Components that matched to on TA-FC

component). To facilitate visualization and interpretation of loading scores, we chose a scaling approach using a modification of the median absolute deviation (MAD): the median absolute deviation about zero ( $MAD_{\mu_0=0}$ ). MAD (Equation 1) is an alternative measure of dispersion to the standard deviation. MAD is a robust measure, being less influenced by large deviations in the distribution compared to standard deviation<sup>4</sup>.

**Equation 1**

$$MAD = \text{median}(|X_i - \text{median}(X)|)$$

Because zero was an absolute null-point in spatial correlation weighting, where there is no metadata association, we used:

**Equation 2**

$$MAD_{\mu_0=0} = \text{median}(|X_i - 0|) = \text{median}(|X|)$$

to calculate the dispersion about zero. Accordingly, we scaled the Disease Loading matrix and the Behavior Loading matrix separately:

**Equation 3:**

$$\text{Disease Loading Score} = \frac{X_i}{\text{Disease Matrix } MAD_{\mu_0=0}} = \frac{X_i}{0.017}$$

**Equation 4:**

$$\text{Behavior Loading Score} = \frac{X_i}{\text{Behavior Matrix } MAD_{\mu_0=0}} = \frac{X_i}{0.020}$$

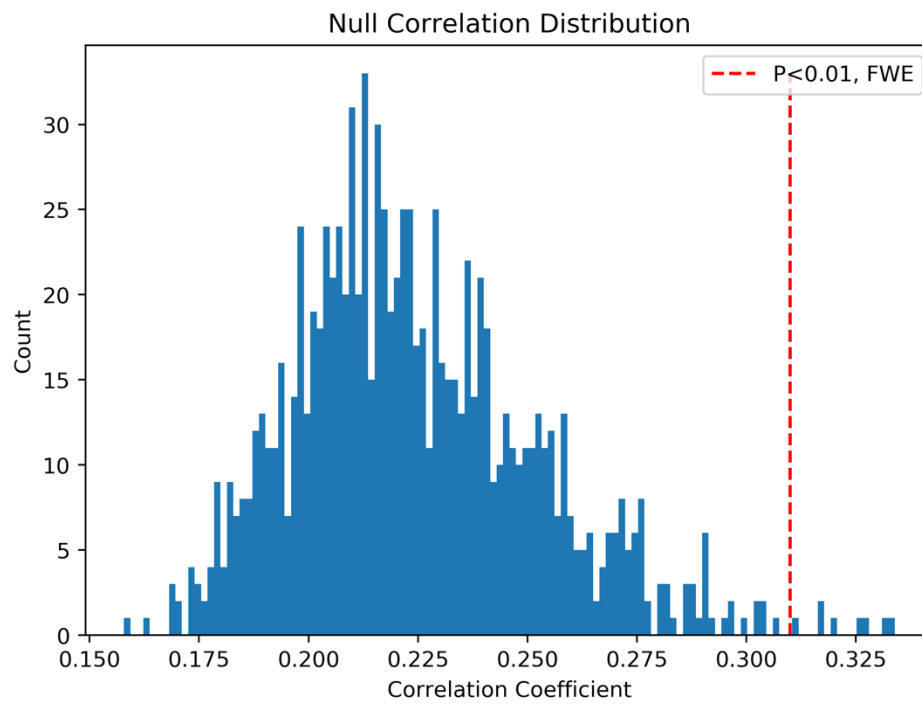
The probability density plots for each metadata loading matrix with scaling marks are shown in Sup. Figure 2.

To help interpret raw loadings, we have provided experiment-level data and corresponding components in Sup. Figure 5.

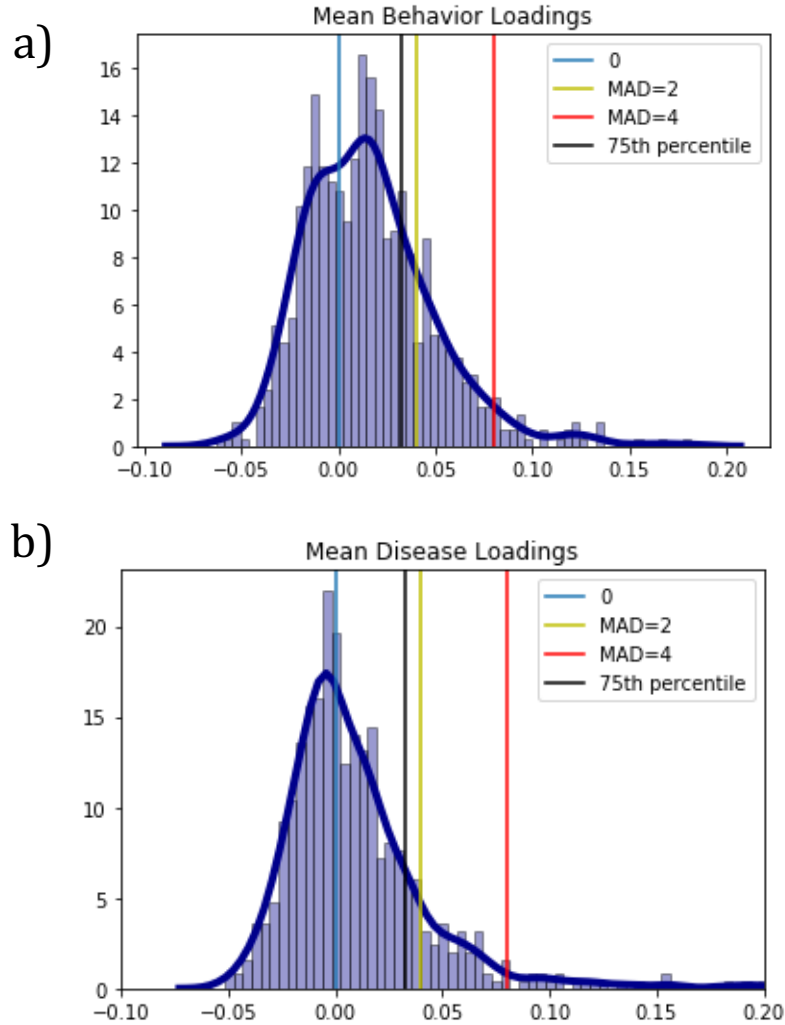
**Metadata Matching Across Modalities.** While spatial matching between networks was evaluated, we also aimed to confirm that Behavior and Disease loadings showed broad overlap across matched networks. To put this broader question in a specific example: does the Behavior category '*Emotion.Reward*' similarly load on the fronto-striatal vbm component as it does to the spatially matched fronto-striatal functional component?

As expected, the correlation coefficient between matched component loading matrices for behaviors ( $r = 0.76$ ,  $\rho = 0.72$ ) and diseases ( $r = 0.8$ ,  $\rho = 0.67$ ) were high. Partial correlations after adjusting for the match-specific magnitude of correspondence between modalities did not appreciably alter the results ( $< 3\%$  in correlation magnitude), which suggests that mismatch in loadings were not systematically driven by weaker spatial matches in any major way. As Sup. Figure 4 demonstrates, both graphs show a slight negative bias: the linear fitted plots are slightly below unity. This means that a metadata association with a network from its opposite modality (i.e., Behavior Loading-VBM Network) is slightly lower than its corresponding modality (i.e., Behavior Loading-Functional Network). This is to be expected as the functional and vbm matches are not perfect, but they show "reciprocal" validity.

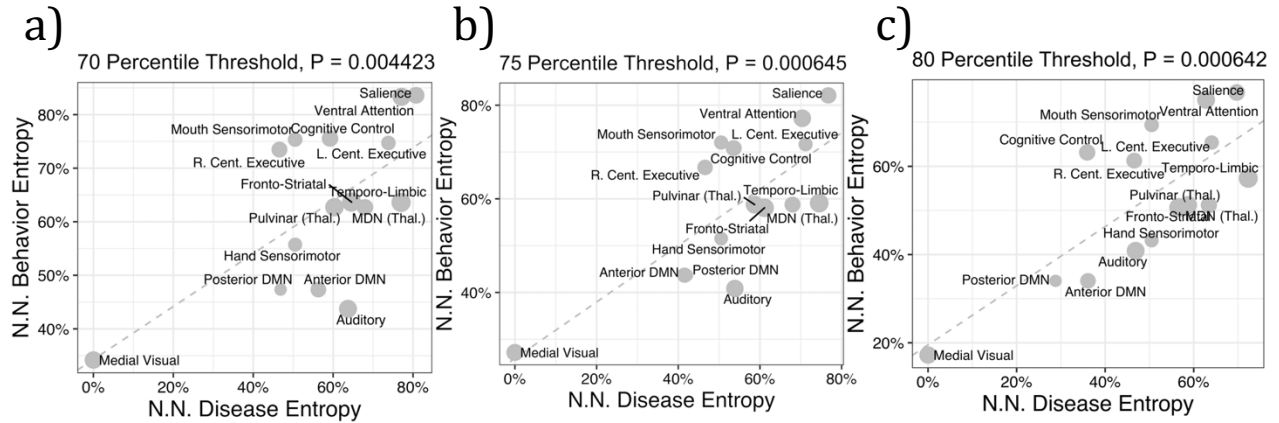
## Supplementary Figures



**Supplementary Figure 1.** In the 1,000 iteration family-wise error rate (FWE) procedure employed here, 20\*1,000 noise images were simulated in total to produce a null-distribution.

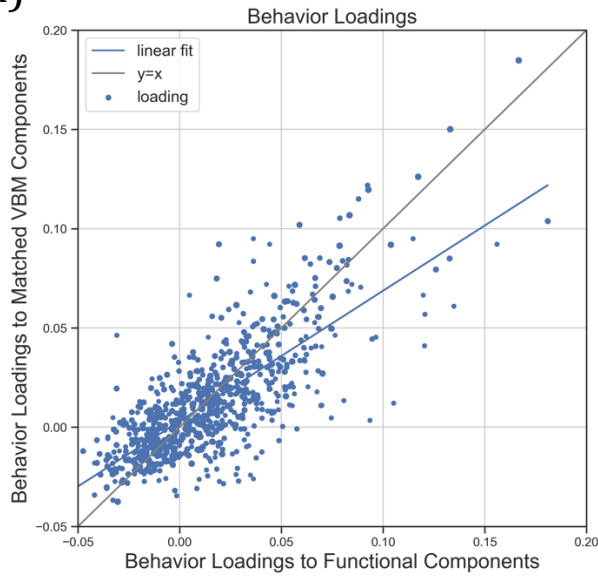


**Supplementary Figure 2a-b.** Probability density plots for the mean metadata-component association correlations (pre-scaled) derived from all  $56 \times 13 = 728$  Behavior-Component mean correlations (a) and  $43 \times 13 = 602$  Disease-Component mean correlations (b). The second median absolute deviation from zero is shown in yellow (i.e., scaling score = 2 in Figure 4). The fourth median absolute deviation from zero is red (i.e., scaling score = 4 in Figure 4). The black line corresponds to the 75<sup>th</sup> percentile, which was chosen for zeroing in our entropy analysis.

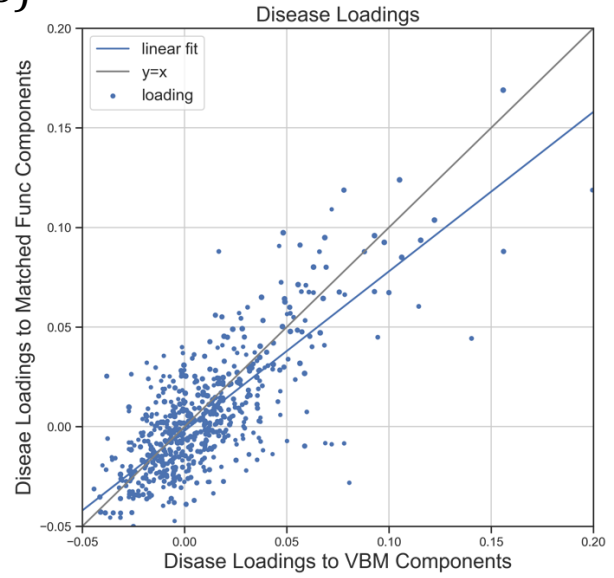


**Supplementary Figure 3a-c.** Disease Entropy vs. Behavior Entropy linear regression plots with corresponding loading thresholds for our entropy measure. To check the stability of our result, alternate thresholds were chosen 5 percentiles below (A) and above (C) our selected threshold (75<sup>th</sup> percentile, B). Each regression remains significant after correcting for multiple tests.

a)



b)

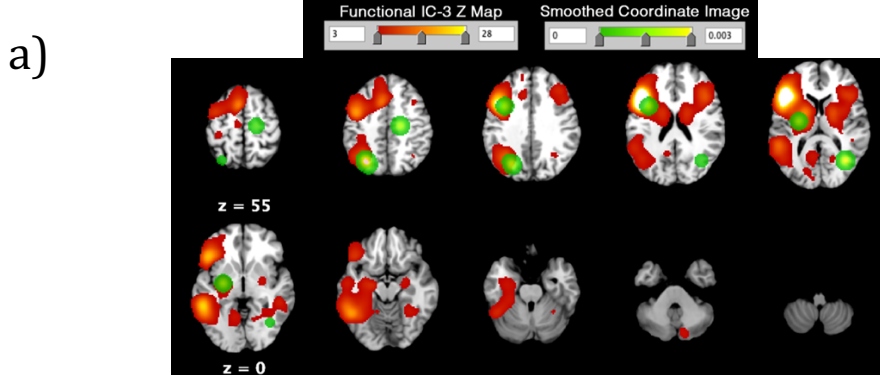


**Supplementary Figure 4a-b.** Reciprocal loadings across modalities. The grey line represents the unity ( $y=x$ ) plot, whereas the blue line corresponds to the linear fit to the data. Both graphs demonstrate a slight negative bias in opposite-modality loading (y-axis).



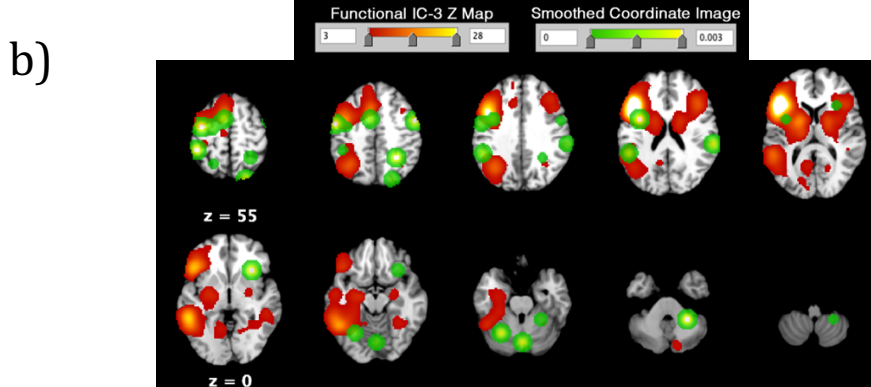
Example A, Experiment 5040011\_3 (BrainMapID\_Exp)  
 $r = 0.156$  (6 foci)

Behavioral Domain(s): *Cognition.Reasoning, Cognition.Attention*



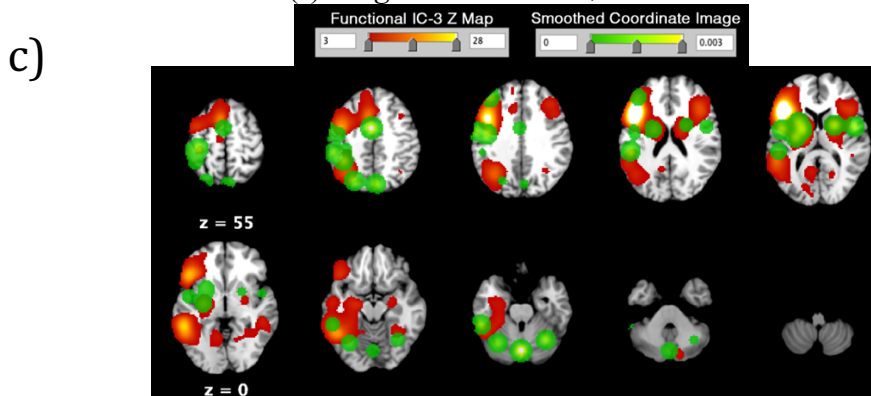
Example B, Experiment 5040007\_1  
 $r = 0.0798$  (16 total foci)

Behavioral Domain(s): *Perception.Audition*



Example C, Experiment 11080075\_1  
 $r = 0.0322$  (16 total foci)

Behavioral Domain(s): *Cognition.Attention, Emotion.Positive.Reward/Gain*



**Supplementary Figure 5a-c.** Experiment-Level correlations between smoothed three coordinate images (a,b,c) and example ICA component map (Functional IC-3).

## Supplementary References

1. Smith, S. *et al.* Structural Variability in the Human Brain Reflects Fine-Grained Functional Architecture at the Population Level. *J. Neurosci.* 39, 6136–6149 (2019).
2. Westfall, P. H. & Young, S. S. *Resampling-Based Multiple Testing: Examples and Methods for p-Value Adjustment.* (Wiley, 1993).
3. Alexander-Bloch, A. *et al.* On testing for spatial correspondence between maps of human brain structure and function. *Neuroimage* (2018). doi:10.1016/j.neuroimage.2018.05.070
4. Leys, C., Ley, C., Klein, O., Bernard, P. & Licata, L. Detecting outliers: Do not use standard deviation around the mean, use absolute deviation around the median. *Journal of Experimental Social Psychology* 49, 764–766 (2013).